

Supplementary Information

Superior cycling stability and high rate capability of three-dimensional Zn/Cu foam electrodes for zinc-based alkaline batteries

Zhao Yan ^{a,b}, Erdong Wang ^a, Luhua Jiang ^a, Gongquan Sun ^{a*}

- a. Division of Fuel Cell & Battery, Dalian National Laboratory for Clean Energy, Dalian Institute of Chemical Physics, Chinese Academy of Sciences, Dalian 116023, China. E-mail: gqsun@dicp.ac.cn Tel: +86-411-84379063
- b. University of Chinese Academy of Sciences, Beijing 100039, China.

Table of Contents

Fig. S1. Schematic diagram of zinc/zinc quasi-symmetric cell.

Fig. S2. Schematic diagram of prototype Zn/Ni battery.

Fig. S3. Photographs and I-V curves of Zn/Cu foam electrodes prepared by different electro-deposition methods.

Fig. S4. Coulombic efficiency of Zn/Cu foam electrodes prepared by different electro-deposition current densities.

Fig. S5. Photographs of Copper foam and Zn/Cu foam electrode.

Fig. S6. X-ray Diffraction patterns of Zn/Cu foam electrodes.

Fig. S7. Electrochemical impedance spectroscopies of Zn/Ni battery after different cycles.

Table. S1. Comparison of the cycling stability of zinc electrodes in zinc/zinc (quasi-)symmetric cells.

Table. S2. Comparison of the cycling stability of zinc electrodes in Zn/Ni secondary batteries.

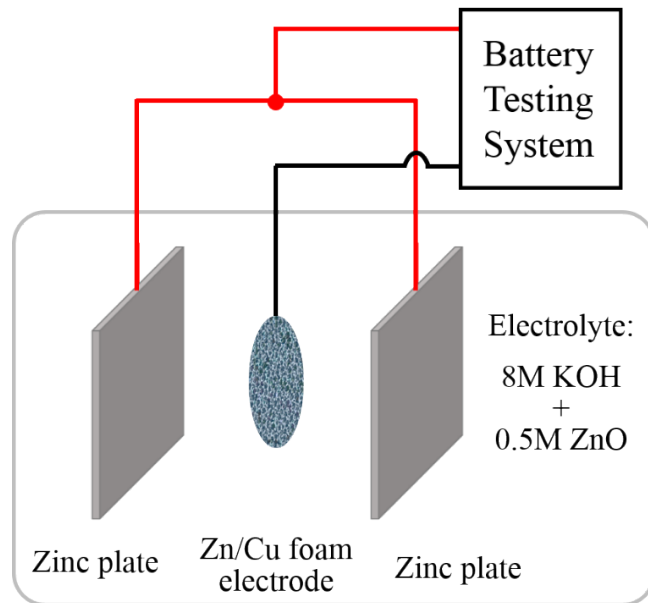


Fig. S1. Schematic diagram for zinc/zinc quasi-symmetric cell.

Current density of Zn/Cu foam electrode is calculated according to both areas of the electrodes. In zinc/zinc quasi-symmetric cell, current density of $250 \text{ mA}\cdot\text{cm}^{-2}$ was adopted to evaluate the cycling stability of zinc electrode. Thus, the actual current of zinc electrode can be calculated as follows:

$$I = \text{current density} \times \text{area} = 250 \text{ mA}\cdot\text{cm}^{-2} \times 2.54 \text{ cm}^2 \times 2 = 1270 \text{ mA}$$

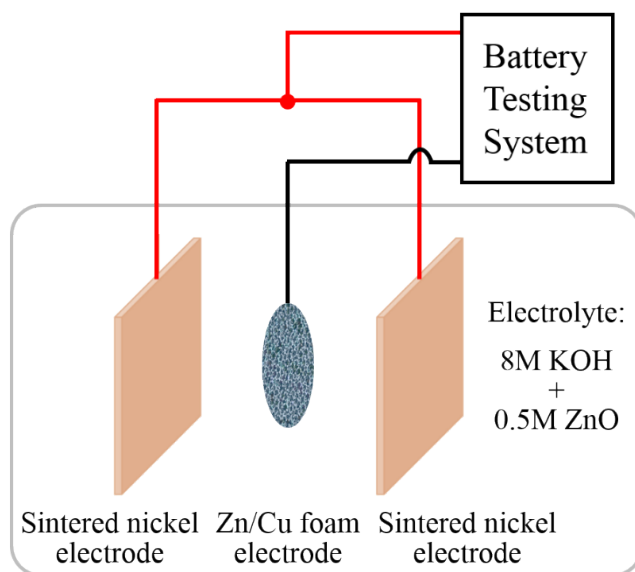


Fig. S2. Schematic diagram for prototype Zn/Ni battery.

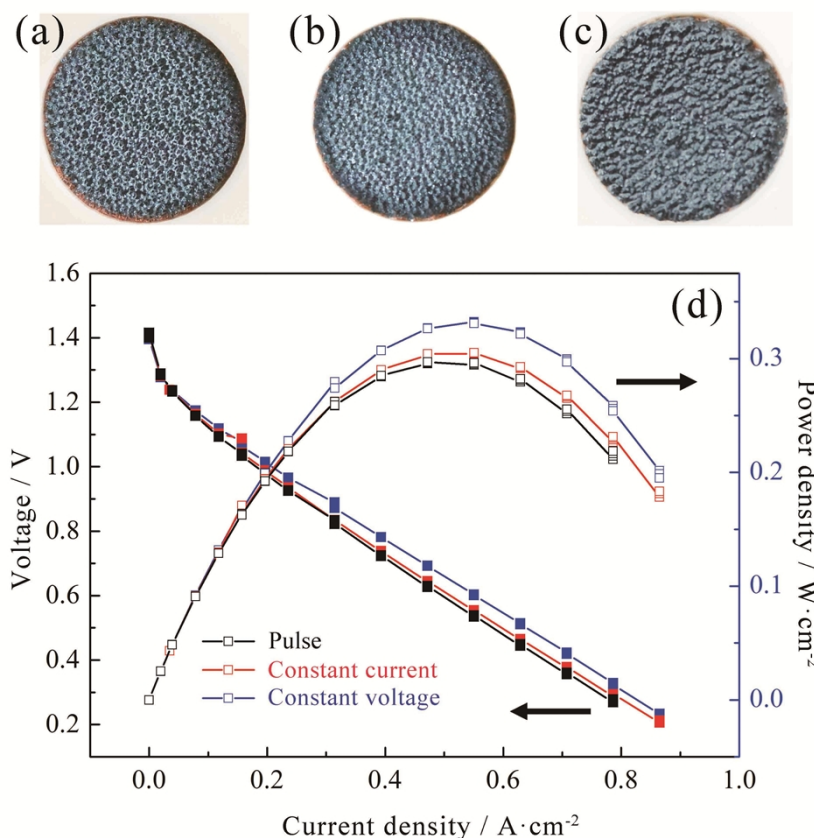


Fig. S3. Photographs and I-V curves of Zn/Cu foam electrodes prepared by different electro-deposition methods. (a) Pulse electro-deposition (current density: $1 \text{ A}\cdot\text{cm}^{-2}$, frequency: 250 Hz, duty ratio: 0.25, zinc loading: 200 mAh); (b) Constant current electro-deposition (current density: $1 \text{ A}\cdot\text{cm}^{-2}$, zinc loading: 200 mAh); (c) Constant voltage electro-deposition (voltage: 1.7V, zinc loading: 200 mAh); (d) I-V curves of zinc/oxygen batteries with Zn/Cu foam electrodes (Electrolyte: $7 \text{ mol}\cdot\text{L}^{-1}$ KOH, cathode: commercial air electrode, O_2 flow rate: 50 sccm).

Different electro-deposition methods were adopted to prepare Zn/Cu foam electrodes. Fig. S3 shows the photographs and I-V curves of these Zn/Cu foam electrodes. Obviously, the electrodes prepared by pulse electro-deposition exhibit the most uniform zinc distribution. Though the peak power density of Zn/Cu foam electrode with constant voltage method is the highest among these methods mainly due to the thick zinc layer on the electrode reduce the distance between zinc electrode and air cathode, pulse electro-deposition is chosen in the following experiments.

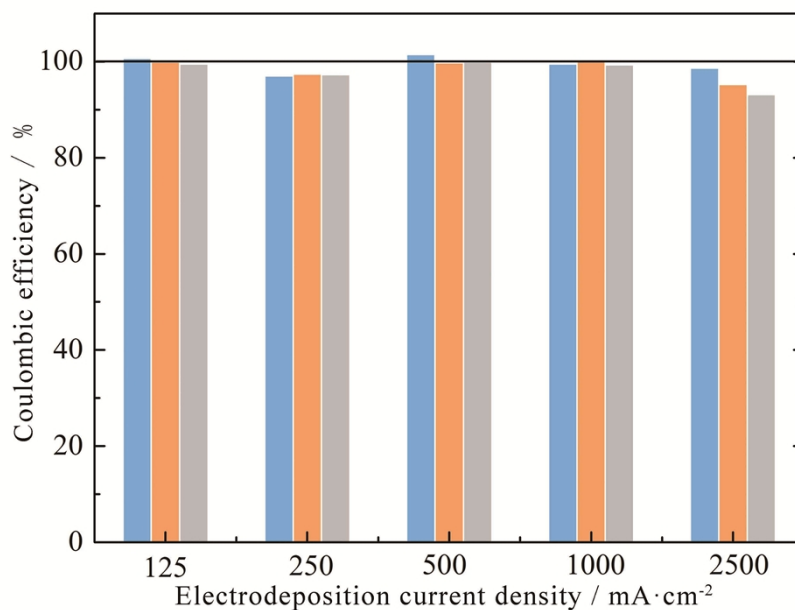


Fig. S4. Coulombic efficiency of Zn/Cu foam electrodes prepared by different electro-deposition current densities (frequency: 250 Hz, duty ratio: 0.25).

Different current densities in pulse electro-deposition method were conducted to screen the best condition. Three electrodes were prepared at each current density to ensure the repeatability. To evaluate the coulombic efficiency, Zn/Cu foam electrodes were weighted after washed in abundant water and dried in N₂. Fig. S4 shows that the electrodes prepared at current density of 125, 500 and 1000 mA·cm⁻² show the highest coulombic efficiency and the best repeatability. Thus, considering the deposition time, 1000 mA·cm⁻² was chosen in the following experiments.

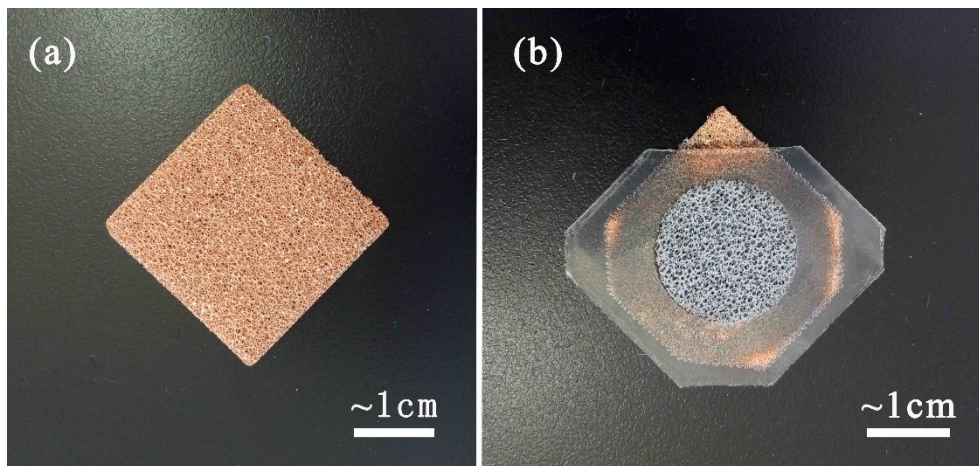


Fig. S5. Photographs of Copper foam (a) and Zn/Cu foam electrode (b).

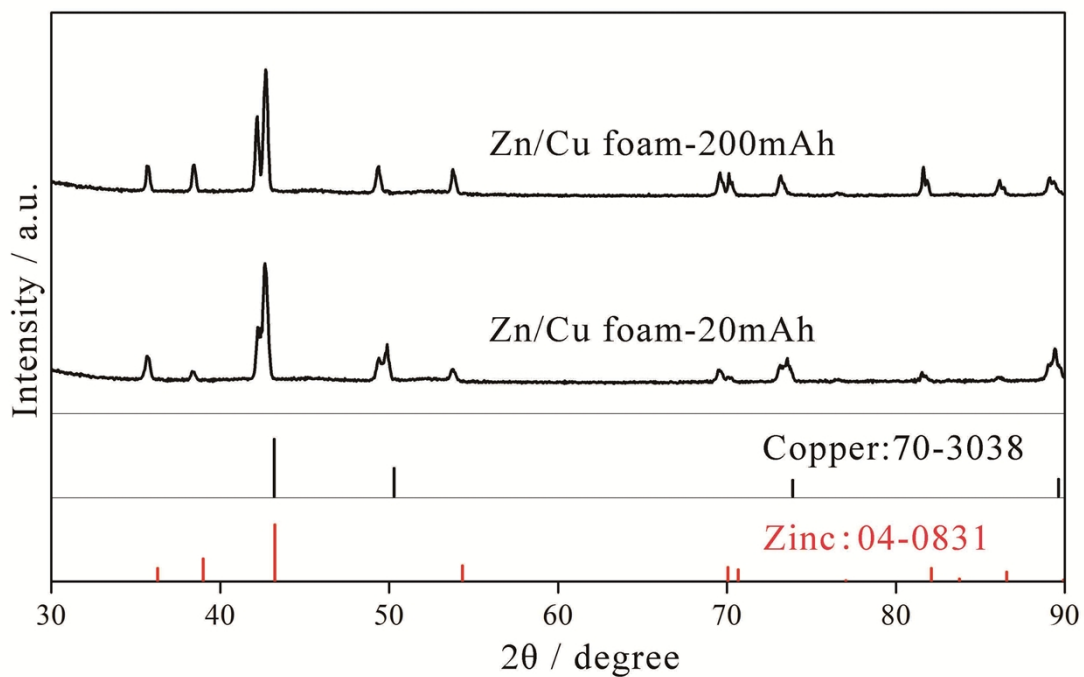


Fig. S6. X-ray diffraction patterns of Zn/Cu foam electrodes.

X-ray diffraction (XRD) patterns of the as-prepared Zn/Cu foam electrodes with zinc loading of 20 mAh (Zn/Cu foam-20mAh) and 200 mAh (Zn/Cu foam-200mAh) were conducted on X'pert Pro (PANalytical) diffractometer (60 kV, 55 mA) using Cu $K\alpha$ radiation at a scanning rate of $2\theta = 5^\circ \text{ min}^{-1}$.

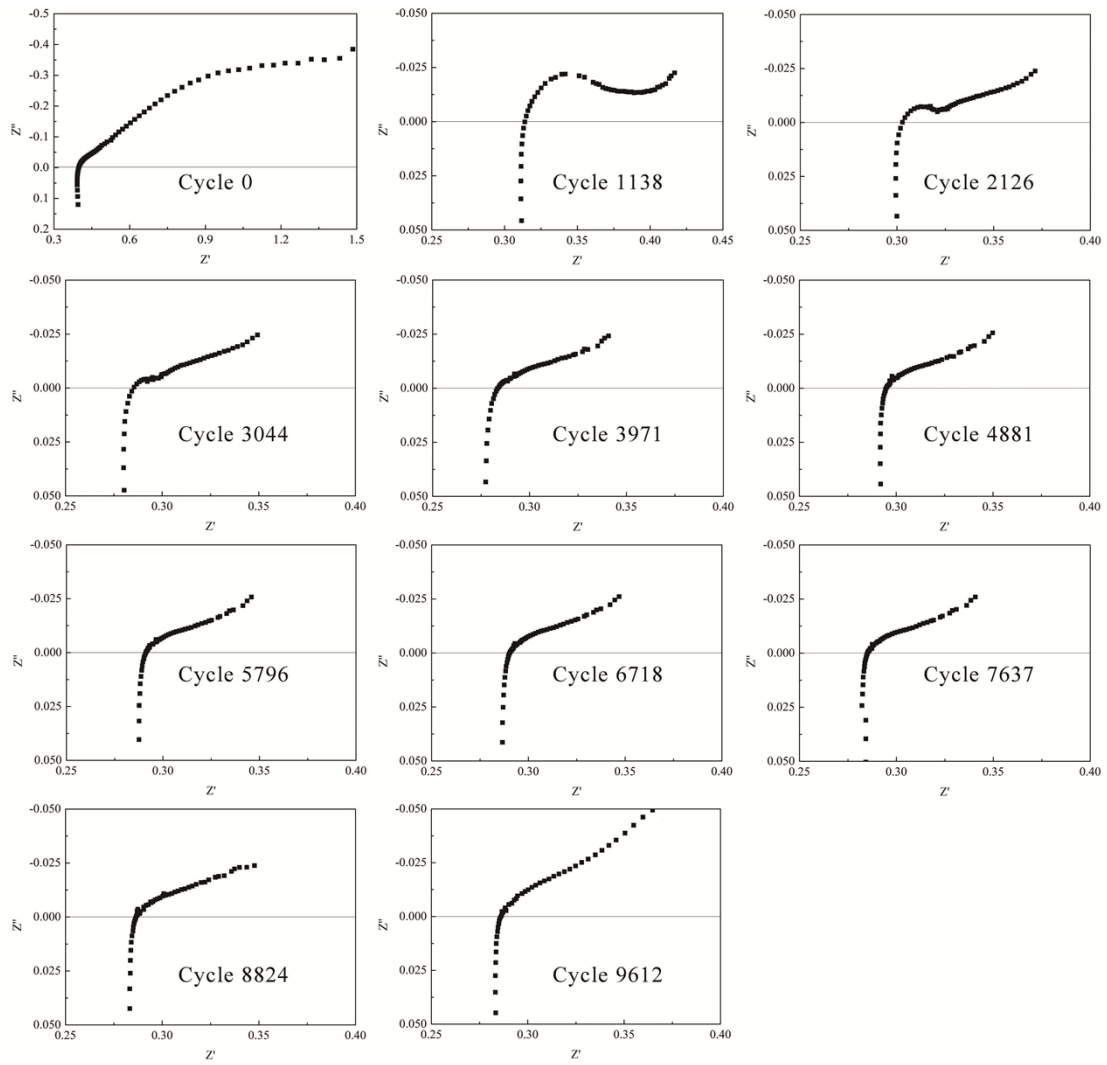


Fig. S7. Electrochemical impedance spectroscopies of Zn/Ni battery after different cycles.

Table. S1. Comparison of the cycling stability of zinc electrodes in zinc/zinc (quasi-)symmetric cells.

Current density/ $\text{mA} \cdot \text{cm}^{-2}$	Depth of discharge	Cycle number	Ref.
250	100%	10,000	This work
24	23%	45	1

Table. S2. Comparison of the cycling stability of zinc electrodes in Zn/Ni secondary batteries.

Current	Discharge capacity retention at maximum cycle number [†]	Ref.
25.4C (100 $\text{mA} \cdot \text{cm}^{-2}$)	97.8%@100th 89.2%@800th 82.2%@9000th	This work
0.3C	35%@160 th	2
0.3C	52.9%@300 th	3
0.2C	95.4%@50 th	4
1C	98.2%@800 th	5
1C	90.9%@100 th	6
0.5C	87%@320 th	7

[†]Discharge capacity retention are calculated based on the maximum discharge capacity instead of the initial discharge capacity.

Supplementary References

1. J. F. Parker, C. N. Chervin, E. S. Nelson, D. R. Rolison and J. W. Long, *Energy Environ. Sci.*, 2014, **7**, 1117-1124.
2. S. H. Lee, C. W. Yi and K. Kim, *J. Phys. Chem. C*, 2011, **115**, 2572-2577.
3. Y. F. Yuan, J. P. Tu, H. M. Wu, Y. Z. Yang, D. Q. Shi and X. B. Zhao, *Electrochim. Acta*, 2006, **51**, 3632-3636.
4. Y. F. Yuan, L. Q. Yu, H. M. Wu, J. L. Yang, Y. B. Chen, S. Y. Guo and J. P. Tu, *Electrochim. Acta*, 2011, **56**, 4378-4383.
5. R. J. Wang, Z. H. Yang, B. Yang, T. T. Wang and Z. H. Chu, *J. Power Sources*, 2014, **251**, 344-350.
6. J. Huang and Z. Yang, *RSC Adv.*, 2014, **4**, 19205-19209.
7. C. Tang, D. Zhou, S. Fang and L. Yang, *J. Electrochem. Soc.*, 2012, **159**, A1796-A1800.